Separation and Purification Technology 247 (2020) 116909

Contents lists available at ScienceDirect

Separation and Purification Technology

journal homepage: www.elsevier.com/locate/seppur

Electrohydromodulation for phosphate recovery from wastewater

Mahamalage Kusumitha Perera (Ph.D.)[a,*], James D. Englehardt (Ph.D.)[a], Joshua L. Cohn (Ph.D.)[b], Edward A Dauer (M.D.)[c], Dharmendra Shukla (M.S.)[b]

[a] Civil, Architectural, and Environmental Engineering, PO Box 248294, Coral Gables, FL 33124-0630, USA
[b] Department of Physics, University of Miami, Coral Gables, FL 33416, USA
[c] Biomedical Engineering, Radiology and Family Medicine, University of Miami, Coral Gables, FL 33416, USA

ARTICLE INFO

Keywords:
Municipal wastewater
Phosphorus
Nutrient recovery
pH modulation
Electrochemical

ABSTRACT

The mining of phosphate rock to produce fertilizer, and subsequent disposal of the municipal wastewater containing a significant fraction of the phosphate applied agriculturally, has led to environmental impacts of phosphate mining as well as surface water eutrophication. However, recovery of phosphate ($H_2PO_4^-$, HPO_4^{2-}, PO_4^{3-}) from wastewater, either chemically or biologically, has not been sufficiently economical at low phosphate concentrations in raw wastewater (~2.4 mg-P l^{-1}) to motivate widespread adoption. In this work, we demonstrate phosphate recovery directly from raw and mineral-spiked septic tank effluent by electrochemical pH shifting, termed electrohydromodulation (EHM), without expensive chemical addition. EHM using a CMI-7000 multivalent cation exchange membrane (MCEM) at 5 V at 1.347 mA/cm^2 resulted in the highest efficiency at lowest energy consumption. 94 and 95% phosphate were recovered from mineral-spiked septic tank effluent (simulating advanced oxidation-based direct potable reuse water), and raw septic tank effluent, at an energy demand of 1.046 kWh/m^3 (3.960 kWh/1000 Gal) and 1.863 kWh/m^3 (7.054 kWh/1000 Gal), respectively, low despite use of non-toxic, inexpensive graphite electrodes. Results from scanning electron microscopy (SEM), energy-dispersive X-ray spectroscopy (EDS) and X-ray powder diffraction (XRD) indicated that recovered precipitates consisted principally of amorphous calcium phosphate (ACP), with minor amounts of amorphous calcium carbonate (ACC), having an overall Ca:P ratio of 2. CO_2 stripping at low pH prior to pH shifting was found to minimize competitive calcite precipitation to improve product purity. Electrodes used intermittently, with polarity reversal, over 1.5 years of experiments were intact from fouling.

1. Introduction

Food production and agriculture today are highly dependent on phosphate fertilizer use, and phosphate strip mines worldwide produce over 280 Mt of radioactive phosphogypsum waste annually [1–4]. On the other hand, phosphate recovery from wastewater can satisfy 15% of phosphorus fertilizer demand [5] and thereby reduce phosphate mining. Thus, although phosphate recovery from wastewater may be economically challenging relative to the current cost of commercial fertilizer, the economics of recovery is favorable when environmental impacts are considered [6,7].

Although many phosphate recovery technologies are available, only some have been recognized as cost effective [8]. For example struvite precipitation can be efficient at high phosphate concentrations, but may not be economical at low phosphate concentrations. Therefore, the development of novel technologies has been recommended [9]. In addition, the energy consumption of the process should be assessed hand in hand, inasmuch as it would affect operating cost as well as carbon emissions of the process. In these aspects, electrochemical phosphate recovery processes have shown promise [10–12].

Electrochemical phosphate recovery has operational advantages over conventional phosphate recovery technologies, because phosphate can be recovered electrochemically without chemical dosing. In contrast, most currently-developed phosphate recovery processes require chemical storage and dosing, which typically requires trained operators [8] as well as regular transportation of chemicals. For example, although adsorption processes do not require chemicals, regeneration of ion exchange and magnetic microsorbent media requires chemicals such as NaCl and NaOH. Electrodialysis generates a concentrated phosphate stream, however phosphate separation would require Mg^{2+} addition [in the form of $MgCl_2$ or $Mg(OH)_2$] for struvite precipitation. Chemical precipitation would require addition of multi-valent metal

* Corresponding author.
E-mail addresses: m.perera@miami.edu (M.K. Perera), jenglehardt@miami.edu (J.D. Englehardt), jcohn@miami.edu (J.L. Cohn), dauer.edward@gmail.com (E.A. Dauer), dpshukla@miami.edu (D. Shukla).

https://doi.org/10.1016/j.seppur.2020.116909
Received 3 September 2019; Received in revised form 18 December 2019; Accepted 22 April 2020
Available online 23 April 2020
1383-5866/

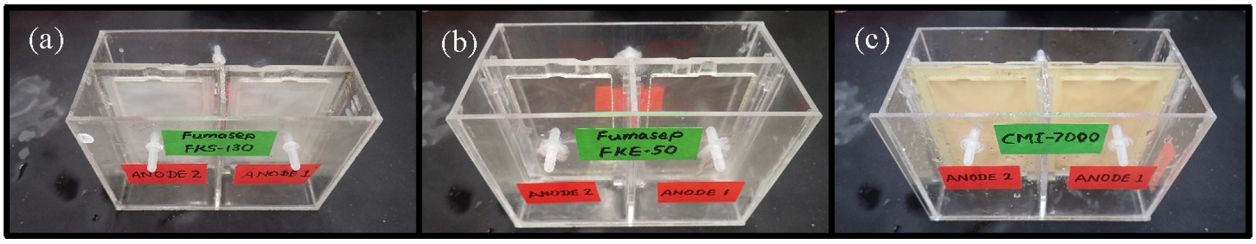

Fig. 1. Electrochemical pH modulating reactors fabricated with different multi-valent cation exchange membranes [(a) Fumasep-FKS-130, (b) Fumasep-FKE-50, (c) CMI-7000].

cations such as Fe^{3+}, Al^{3+} and Ca^{2+}.

Chemical free processes are particularly preferred in decentralized treatment plant applications [8], such as net-zero water plants which are economical at plants serving as few as 100 – 1000 homes [13]. For example, although biological phosphorous recovery processes can be operated without continuous chemical dosing, the process is sensitive to shock loadings, and separation of phosphate would involve struvite precipitation with Mg^{2+} addition. Also, although electrocoagulation can electrochemically dose Fe^{3+}, Al^{3+} for phosphate precipitation, the process is sensitive to pH, and chemical pH adjustment may be required [14]. In contrast, electrochemical processes can produce a marketable fertilizer product requiring minimal post-processing [8].

Electrochemical processes for phosphate recovery typically employ sacrificial anodes to dose cations such as Mg^{2+}, Al^{3+}, Fe^{2+} or Fe^{3+}, to support chemical precipitation [14–17]. Among these, electrochemical Mg^{2+} dosing has become popular for inducing struvite precipitation, as a more cost-effective alternative to Mg^{2+} supplementation using $MgSO_4$, MgO, $Mg(OH)_2$, $MgCl_2$ [15]. However the process is effective only on concentrated phosphate streams such as urine [15] and anerobic sludge digester supernatant [18], because low phosphate streams require a pH higher than 9 [19,20]. Hug and Udert [15] indicated that the process is economical compared with the addition of rapidly-dissolving chemicals such as $MgCl_2$ or $MgSO_4$, but more expensive than adding slowly-dissolving MgO.

As an alternative to the use of sacrificial anodes, the use of dimensionally-stable anodes (DSAs ®) coupled with recently developed cation exchange membranes (CEMs), has been shown for the adjustment of process pH to support precipitation [10–12,21]. Because aqueous pH exerts a dominant influence on reactions in water, such an in-situ process can avoid the cost of chemical addition [22], as well as the expenditure of energy required for their production, in many applications. That is, the pH of water can be shifted electrochemically, through electrolysis:

$$\text{Anode: } 2H_2O \rightarrow 4H^+ + O_2 + 4e^- \quad (1)$$

$$\text{Cathode: } 4H_2O + 4e^- \rightarrow 4OH^- + 2H_2 \quad (2)$$

Kappel et al. [10] demonstrated over 90% phosphate precipitation and recovery from membrane bioreactor (MBR) nanofiltration concentrate (derived from a membrane bioreactor) by shifting the pH above 9 electrochemically. However the aerobically-treated and nanofiltered domestic wastewater inflow to the process of Kappel et al. [10] contained only 1.63 mg l^{-1} PO_4^{3-} as P, whereas medium-strength domestic wastewater contains ~ 2.4 mg l^{-1} inorganic phosphorous prior to treatment [23]. More recently Cid et al. [12] showed phosphate recovery from toilet wastewater, much more concentrated (18.6 mg-P l^{-1}) than typical domestic wastewater. However, that process was run without the use of a CEM, at a high energy demand, and the authors indicated that precipitate formation on the cathode surface may be problematic in long term operation.

Electrochemical processes are potentially more efficient for treatment of more highly mineralized waters. For example, we recently demonstrated an economical, advanced oxidation-based net-zero water treatment system, i.e., a nearly closed-loop direct potable water reuse system [24,25] which, because minerals are not substantially removed, maintains a total dissolved solids concentration on the order of 500 mg l^{-1}. Such water has higher specific conductance, potentially avoiding ohmic losses in an electrochemical process.

The purpose of this work is to demonstrate efficient phosphate-recovery, directly from raw septic tank effluent and hence prior to microbiological assimilation into biomass, by electrochemical pH shifting, termed electrohydromodulation (EHM). In particular, the results of bench-scale experiments using EHM to recover phosphate from simulated and real septic tank effluent, with and without mineral spiking to simulate the influent to a net-zero water (NZW) process. The EHM process used in this application employs a CMI-7000 multi-valent cation exchange membrane to allow pH shift across a small electrode gap, while minimizing neutralization due to proton exchange. Recovered phosphate precipitates were analyzed and characterized using SEM, EDS and XRD techniques. The optimum voltage for the EHM reactor voltage was determined considering the phosphate recovery efficiency and corresponding energy use, as the groundwork for a continuous-flow nutrient recovery system.

2. Materials and methods

2.1. pH modulation reactor construction

Three pH modulating reactors were fabricated using proprietary Fumasep-FKS-PET-130 [polyethylene terephthalate (PET) reinforced], Fumasep-FKE-50 (non-reinforced) and CMI-7000 MCEMs (gel polystyrene cross linked with divinylbenzene having sulphonic acid functional groups), as shown in Fig. 1, a, b & c respectively. The reactors were built with Plexiglass (polymethyl methacrylate) using plastic weld to glue the plexiglass sheets and silicone sealant to prevent leaks. Anode compartments were divided into two with a Plexiglass sheet, such that each reactor comprised three compartments: Anode 1 (front right), Anode 2 (front left) and Cathode (back) (Fig. 1). Two 10.16 × 7.62 × 0.3175 cm (4″x3″x1/8″) isomolded graphite plate electrodes (Fuel Cell Store, USA) were used as anodes, and a 10.16 × 15.24 × 0.3175 cm (4″x6″x1/8″) isomolded graphite plate electrode (Fuel Cell Store, USA) was used as the cathode. The MCEMs in each anode compartment had an effective surface area of 54.4 cm^2 (3.75″x2.25″), mounted in Plexiglas frames which were centered in the 10 mm gap between the anodes and the cathode. Anode 1, Anode 2 & Cathode compartments had working volumes of 300, 300 & 575 mL, and the corresponding holding tanks had working volumes of 1700, 1700 & 1425 mL respectively.

2.2. Reactor operation

The pH modulation reactors were operated in batch mode (Fig. 2), in such a way as to simulate a continuous-flow operation in which influent is introduced to Anode 1 compartment, passed through the Cathode compartment, and discharged after passing through the Anode 2 compartment. That is, the three reactor compartments and the corresponding holding tanks were filled initially with ~ 2 L of test water,

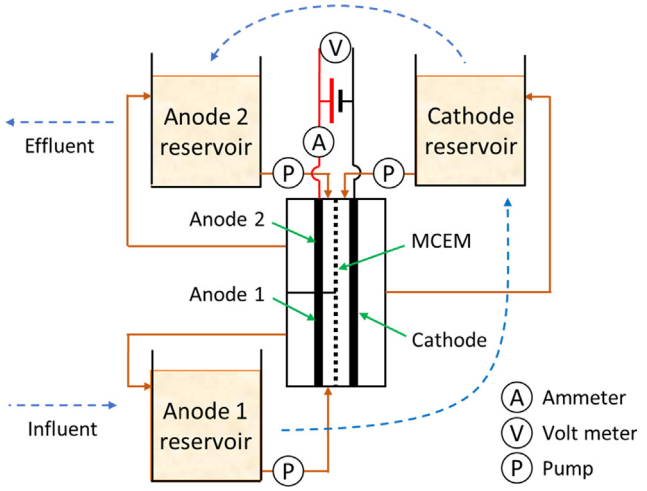

Fig. 2. Schematic diagram of the electrohydromodulation apparatus.

and the reactor was operated in batch mode to produce initial Anode 1, Anode 2 and Cathode solutions. Then, Anode 1 and Cathode solutions just prepared were transferred to Cathode and Anode 2 compartments, respectively (as indicated in dashed arrows in Fig. 2). A new batch of fresh test water was used as the starting Anode 1 (as the influent in continuous-flow configuration) solution, and the Anode 2 solution obtained at the end of the initial experiment was discarded after testing. All batch experiments were conducted as such unless otherwise specified. Unless otherwise stated, all batch experiments were conducted until Anode 1 pH experienced a sharp drop indicating the loss of carbonate buffering in the influent.

Samples of ~ 15 mL at evenly spaced time intervals were withdrawn from each compartment during the experiments, and tested for pH & conductivity and returned to the corresponding compartments to minimize the changes to the volume. Initial and every other sample from the Cathode compartment was kept (not returned to the corresponding compartment) for phosphate analysis. A power supply (BK Precision 1902) was used to supply a constant DC voltage to the electrodes, and multi-meters were used to measure the current through the circuit and voltage between the electrode plates.

2.3. Optimization of cell voltage

Voltage optimization experiments were carried out using synthetic wastewater in the reactor fabricated with Fumasep-FKS-130 MCEM. Synthetic wastewater was prepared by mixing stock solutions in deionized water to simulate the mineral composition of the septic tank effluent from a NZW treatment plant. Stock solutions were prepared using K_2SO_4 (Mallinckrodt), KNO_3 (Mallinckrodt), $NaHCO_3$ (EMD Millipore), $MgCl_2{\cdot}6H_2O$ (BDH Chemicals), NH_4Cl (BDH Chemicals), KH_2PO_4 (BDH Chemicals), $CaCl_2{\cdot}2H_2O$ (Sigma-Aldrich). The composition of the synthetic wastewater is shown in Table 1. β-$Ca_3(PO_4)_2$ (β-tri-Calcium phosphate) (Sigma-Aldrich) was used as seed crystal. ACS or analytical grade chemicals were used in all experiments.

Nominal power supply voltages to be tested were set at 3.5, 5, 7, and 10 V, with an ammeter in series with the anode. Actual voltages between the electrode plates were measured and recorded during experimental runs. During voltage optimization experiments with synthetic wastewater, the polarity of the electrodes was reversed for 3 min every 30 min, with the exception that in 3.5 V experiments the polarity was reversed for 5 min every 30 min. Also, 10 mg of β-$Ca_3(PO_4)_2$ seeds, which is less soluble than amorphous calcium phosphate (ACP), were added to the Cathode compartment after the pH exceeded 7, to act as a precipitate seed. Seed crystals were added only in voltage optimization experiments, so that this addition would not affect the composition of the precipitates recovered from raw and mineral-spiked septic tank effluent.

Table 1
Synthetic Net-Zero Water Septic Tank Effluent Composition.

Ion	Concentration (mg l^{-1})
Ca^{2+}	70.0
Mg^{2+}	12.4
K^+	90.5
Na^+	145
NH_4^+ (as N)	53.3
PO_4^{3-} (as P)	11.7
SO_4^{2-} (as S)	27.9
NO_3^- (as N)	0.54
Cl^-	142
Alkalinity (as $CaCO_3$)	319

2.4. Comparison of MCEMs

Membrane comparison experiments were carried out using mineral-spiked septic tank effluent to simulate NZW septic tank effluent, using the three reactors fabricated as described in section 2.1. The mineral composition of the septic tank effluent and of the mineral-spiked septic tank effluent are shown in Table 2.

2.5. Analysis of precipitates

Precipitates recovered from synthetic wastewater were observed under SEM to study the size and morphology of the precipitates. Micrographs were obtained using FEI/Philips XL-30 Field Emission SEM. The elemental composition of the precipitates was obtained by EDS using scanning electron microscope (JEOL JSM 6010PLUS/LA) at 15 kV and 10 mm working distance. The mineral composition of the precipitates was analyzed based on XRD patterns obtained by diffractometer (Phillips X'Pert MPD) using Cu radiation, using a generator power of 45 kV, 25 mA, a step size of 0.02 Deg, and a scan rate of 8 s/step. QualX version 2.23 software and the PowCod Inorganic 1710 database were used in the analysis of XRD patterns.

Precipitates obtained during voltage optimization experiments were analyzed using SEM imaging to identify the morphology of the precipitates. Both seeded and non-seeded samples were analyzed for comparison.

Precipitates obtained using settled septic tank effluent (without mineral spiking or seeding) were used in the analysis of mineral composition (by XRD) and the elemental composition (by EDS). Precipitates for XRD and EDS analysis were generated using the CMI-7000 membrane. Initially (sample of 02/19/18), all compartments were filled with raw septic tank effluent. Subsequently, the Anode 1 solution resulting from the experiment of 02/19/18 was used as the initial cathode solution in the experiment of 02/20/18, after which the Anode 1 solution resulting from the experiment of 02/20/18 was used as the initial Cathode solution for the experiment conducted on 02/22/18. The

Table 2
Composition of Raw and Mineral-Spiked Septic Tank Effluent.

Ion	Raw septic tank effluent (mg l^{-1})	Mineral-spiked septic tank effluent (mg l^{-1})
Ca^{2+}	19.4 ± 0.6	58.1 ± 1.0
Mg^{2+}	5.4 ± 0.3	11.1 ± 0.3
K^+	16.0 ± 0.2	78.0 ± 6.1
Na^+	52.0 ± 1.2	97.0 ± 2.7
PO_4^{3-} (as P)	4.0 ± 0.5	5.6 ± 0.2
Alkalinity (as $CaCO_3$)	189.8	183.1 ± 9.4

± indicate one standard deviation of replicate measurements.

polarity of the reactor was reversed for 5 mins after 2.5 hrs and at the end of the experiment. This procedure was designed to simulate a continuous-flow reactor configuration. All precipitates were recovered by centrifuging the settled precipitates and drying at 103 ± 2°C.

2.6. Voltammetry experiments

Cyclic voltammetry experiments were conducted on synthetic wastewater having a composition as indicated in Table 1, using an iso-molded graphite electrode, the same electrode material used in the reactor of Fig. 1. The potential was swept from −800 to 1300 mV, at a 100 mV/s scan rate, using a potentiostat (Pine Research WaveDriver 20). An Ag/AgCl reference electrode and a platinum coil counter electrode were used in the experiment.

2.7. Analytical methods

Specific conductance, pH, and temperature were measured by multiprobe (Orion STAR A329). Samples were analyzed for phosphate using the Hach high range (0.33–33 mg-P l^{-1}) total reactive phosphorus TNT reagent set using Method 8114, by UV–visible spectrophotometer (Beckman Coulter DU 720). The Hach phosphate test kit measured all inorganic phosphates ($H_2PO_4^-$, HPO_4^{2-}, PO_4^{3-}) as PO_4^{3-}. Initial test water and samples taken during experiments with synthetic and actual wastewater were filtered using 0.2 and 0.45 μm meter syringe filters (VWR), respectively, before analyzing for phosphate. Cations were analyzed by atomic absorption (Perkin Elmer AAnalyst 800). Samples were acidified with concentrated HNO_3, and dilutions were prepared with 1% HNO_3. Because an air-acetylene flame was used in cation analysis, excess lanthanum (Sigma-Aldrich) was added to the samples to prevent interferences from phosphate. All precipitates from the reactor were dried at 103 ± 2°C. Experiments were carried out in triplicates unless otherwise stated.

3. Results

3.1. Voltage optimization results

Results of the experiments carried out with synthetic wastewater to select an optimum voltage are shown in Fig. 3. The slow change in pH of the Anode 1 compartment indicates the buffering of pH by the influent alkalinity. That is, anode 1 pH was buffered due to the consumption of H^+ produced at the anode, by reaction (3), as the reaction is reverse biased. The loss of alkalinity buffering can be observed in the 7 V experiment (Fig. 3). A sharp drop in anode pH was observed after 0.8 h, which indicated that bicarbonate in the influent was exhausted. Experiments were carried out until the buffering from the alkalinity was lost, except in the case of the 3.5 V experiment which was stopped after 360 mins due to sluggish kinetics.

$$H_2CO_3^* \rightleftharpoons H^+ + HCO_3^- \quad (3)$$

in which

$$H_2CO_3^* \rightleftharpoons H_2CO_{3\,(aq)} + CO_{2\,(aq)} \quad (4)$$

In contrast, the cathode pH shifted rapidly up to pH 9, increasing more slowly thereafter, consistent with the logarithmic pH scale and with the buffering effect of reactions (5) & (6):

$$HPO_4^{2-} \rightleftharpoons H^+ + PO_4^{3-} \quad (5)$$

$$NH_4^+ \rightleftharpoons H^+ + NH_{3(aq)} \quad (6)$$

An optimum voltage for pH modulation was selected based on recovery efficiency and energy requirement. Even though 85.8% of phosphate were recovered with only 0.64 kWh/m^3 in 3.5 V experiments, the reaction kinetics were sluggish for practical purposes as pH only shifted to 9.77 ± 0.07 even after 360 mins (Table 3). On the other hand, as discussed in the next section, higher voltage produced smaller precipitate particles, potentially hindering separation. Therefore 5 V was selected as optimum voltage for the process considering the recovery efficiency and corresponding energy use.

3.2. Precipitates obtained at different voltages

The SEM micrographs of precipitates obtained using synthetic wastewater and shown in Fig. 5 had a round irregular shape, indicating that the precipitates had an amorphous morphology. It can be clearly seen that the size of the precipitates was reduced as the voltage was increased, a result attributed to the reduction in reaction time with increasing voltage. The bulk pH was shifted rapidly at higher voltages, increasing the supersaturation ratio which leads to higher rates of nucleation. On the other hand, lower supersaturated conditions result at low voltages allowing larger crystalline growth [26]. Based on the size of the precipitates formed [Fig. 5 (b)] precipitates would need to be separated by microfiltration (which retains particles > 0.1 μm) when operating at the optimum voltage of 5 V. The background crystalline surface seen in Fig. 5 b & c corresponds to the β-$Ca_3(PO_4)_2$ seed crystals (Fig. 4). Precipitate formation on seed crystals are apparent in seeded samples (b & c in Fig. 5), indicating seed crystals acted as a surface for precipitate nucleation.

3.3. MCEM comparison

Results of MCEM comparison experiments indicated that 90% phosphate removal was achieved just after 1 h of operation at 5 V, regardless of the membrane used (Fig. 6). Fumasep-FKS-130 and Fumasep-FKE-50 produced very similar results in terms of cathode pH, while CMI-7000 produced slightly higher pH under the same conditions. The lowest cathode pH resulted from use of the Fumasep-FKE-50 membrane, which had a higher hydroxyl ion transfer rate (200–500 μmol/(min·cm^2) compared with the Fumasep-FKS-130 membrane [10–30 μmol/(min·cm^2)]. Hence, more hydroxyl ion migration can be expected at the steep pH gradient across the Fumasep-FKE-50 membrane, lowering the energy efficiency of pH modulation. It should be noted that the Fumasep-FKE-50 membrane was very thin compared with the other two membranes, and failed after three experiments at the seal near the plexiglass frame. The similar results produced with all three MCEMs indicates the robustness of the process, and the independence of phosphate recovery with respect to the MCEM used.

The performance of MCEMs was also assessed by the cation migration efficiency (CME), defined as follows:

$$\eta_j = \frac{C_{j,i} - C_{j,f}}{C_{j,i}} \times 100\% \quad (7)$$

in which:

η_j = migration efficiency of j^{th} cation

$C_{j,i}$ = initial concentration of j^{th} cation in Anode 1 compartment

$C_{j,f}$ = final concentration of j^{th} cation in Anode 1 compartment

Fig. 7 shows the initial and final concentrations of Ca, Mg, K, Na, and the migration efficiency of each cation. Results indicate that Fumasep-FKS-130 had the highest CME. The CME of Fumasep-FKE-50 was lowest except with respect to Na^+, and CMI-7000 presented a moderate CME.

The measured energy consumption of the process using different MCEMs was similar, as shown in Table 4. While the phosphate recovery of the CMI-7000 MCEM was slightly low compared to other membranes, mineral analysis indicated that the Ca^{2+} concentration of the influent wastewater was slightly low compared to the wastewater used with the other two membranes, and this likely caused the slightly low phosphate removal. Thus, phosphate removal appeared to be a function of Ca^{2+} and wastewater pH. Also, although Fumasep-FKS-130 allowed

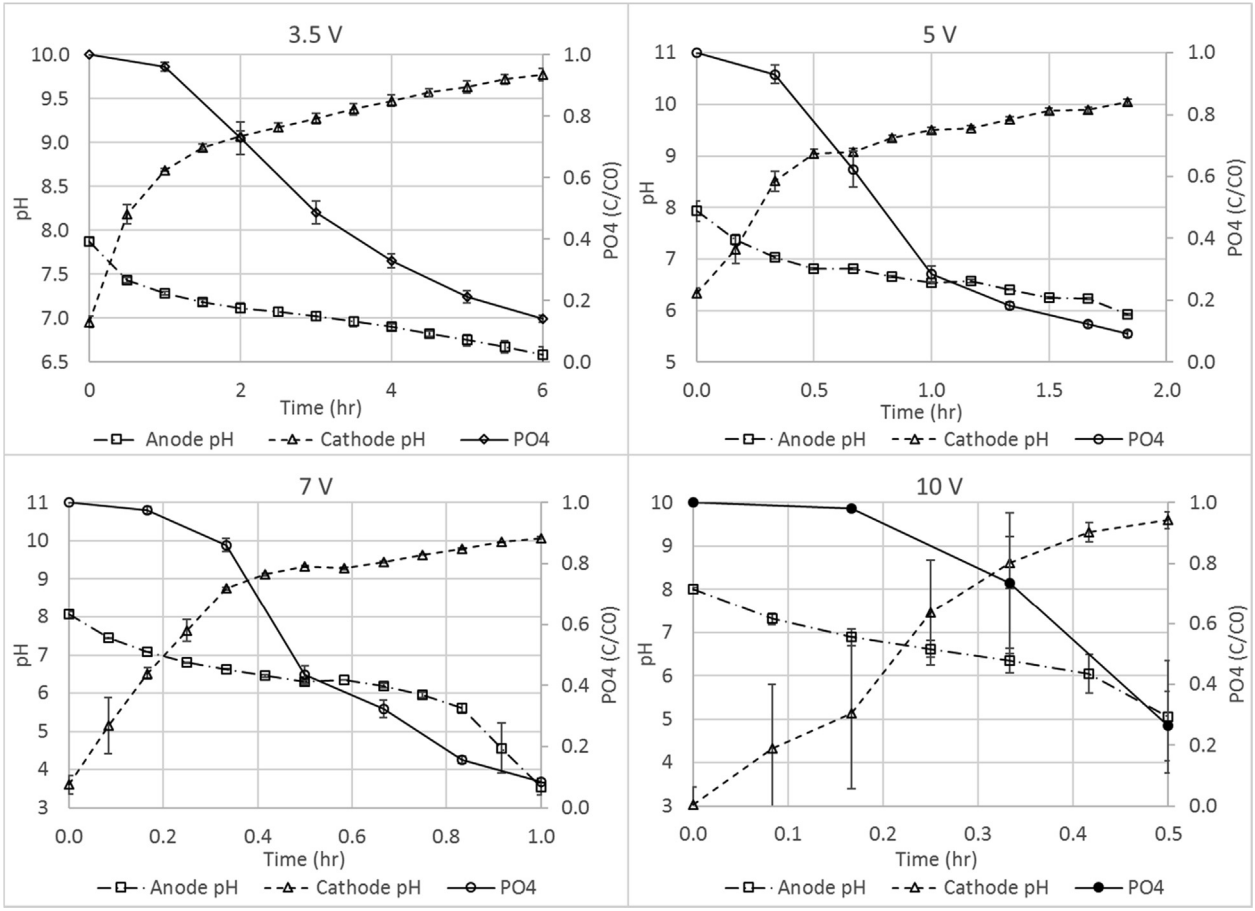

Fig. 3. Results for phosphate recovery experiments at different voltages [Test water: synthetic wastewater; membrane: Fumasep-FKS-130, C_{0,PO_4}~11.75 mg − P l^{-1}].

more Ca^{2+} to migrate through the membrane, only the cathode pH would be expected to affect the phosphate recovery in a continuous-flow reactor, because all Ca^{2+} remaining in the Anode 1 cell would enter the cathode compartment regardless of the mass of Ca^{2+} transferred through the membrane. Hence, the CMI-7000 membrane was selected for the process due to the high cathode pH and low energy consumption.

It should be noted that the use of MCEM greatly reduced the energy consumption and electrode area requirement compared with previous work on electrochemical phosphate recovery. For example, Cid et al. [12] demonstrated phosphate recovery from toilet wastewater (i.e. black water) and reported an energy consumption of 30 ± 5 kWh/m^3. The process required 34 m^2/m^3 of electrode surface area to achieve 60% phosphate removal in 2 hrs. However, in this work 94% phosphate removal was achieved within 2 hrs using mineral-spiked septic tank effluent with only 7.74 m^2/m^3 electrode surface area using 1.046 kWh/m^3 of energy, and 95% phosphate removal was achieved in raw (non-mineral-spiked) septic tank effluent with the same electrode surface area using 1.863 kWh/m^3 in 6 hrs (results shown in Fig. 8).

As described in section 2.5, precipitate analysis experiments were carried out without mineral spiking or seeding. The reactor had to be run for about 6 hrs instead of 2 h at 5 V to reach the end of bicarbonate buffering, because the conductivity of the settled raw septic tank effluent (904 ± 17 µS/cm) was 36% lower than mineral-spiked septic tank effluent (1414 ± 106 µS/cm).

Fig. 8 shows the conductivity of each electrode compartment. Anode 1 conductivity fell linearly up to 5.5 hrs of treatment time, indicating that the cations had migrated to the Cathode compartment. This result is also supported by data shown in Fig. 7. The Anode 1 conductivity increased slightly in the 6 hr sample because of the increased H^+ concentration as the pH dropped to 3.93. Cathode conductivity was mostly stable during the first 2 hrs of the experiment, indicating phosphate precipitation together with migration of Ca^{2+}. After 2 hrs, Cathode conductivity increased linearly as the cations migrated and OH^- was constantly generated at the Cathode. Anode 2 conductivity remained mostly stable up until 4 hrs, due to the buffering

Table 3
Orthophosphate Removal and Energy Consumption at Different Voltages Using Synthetic Wastewater.

Voltage (V)	Average voltage[a] (V)	Average current (mA)	Current density (mA/cm^2)	Time[b] (min)	Energy per 1 m^3 (kWh/m^3)	Energy per 1000 Gal (kWh/1000 Gal)	Final cathode pH[c]	Phosphate recovery %
3.5	3.41	59	0.38	360	0.606	2.293	9.77 ± 0.07	83.2
5	5.01	203	1.31	110	0.934	3.536	10.05 ± 0.05	90.2
7	6.79	427	2.76	60	1.450	5.489	10.43 ± 0.50	93.8
10	9.56	780	5.04	30	1.865	7.061	9.66 ± 0.18	78.7

[a] Voltage between the electrode plates.
[b] Duration of the experiment.
[c] Bounds are ± 1 standard deviation of triplicate (for 3.5 & 5 V) and duplicate (7 & 10 V) measurements.

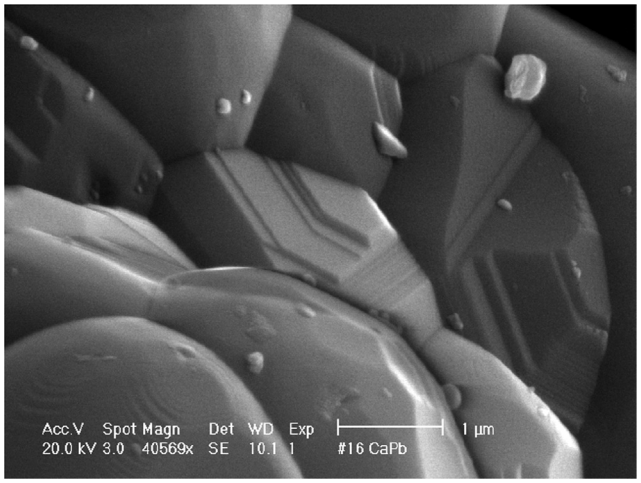

Fig. 4. Laboratory grade β-$Ca_3(PO_4)_2$ seed crystals before use in experiments with synthetic wastewater.

of the remaining fine phosphate and carbonate precipitates in the solution. The conductivity of Anode 2 started decreasing after all the remaining precipitates were dissolved and the buffering capacity of the solution was lost.

The energy consumption of the process increased by 78% in these experiments due to the lower conductivity of raw septic tank effluent. Power consumption for raw septic tank effluent was calculated as 1.863 kWh/m^3 (7.054 kWh/1000 Gal). However the phosphate recovery rate reached 95% at after 5 hrs. The slight increase in phosphate in the 3- & 4-hr samples was probably caused by the dissolution of precipitates formed on the Cathode electrode surface during the polarity reversal at 2.5 hrs. However only a small portion of the precipitates were formed on the cathode compared with the results of Cid et al. [12], in which precipitates formed principally on the cathode surface.

3.4. XRD analysis of the precipitates

XRD analysis of recovered precipitates indicated the presence of calcite [$Ca(CO_3)$], and/or $Mg(OH)_2$ in the samples (Fig. 9). However, no distinct peaks for calcium phosphate precipitates nor any other crystalline minerals (e.g. hydroxyapatite) were observed, indicating that precipitated calcium phosphate mineral(s) had an amorphous morphology or represent a volume fraction that is below detection. Similar precipitate morphology was observed by Kappel et al. [10], who indicated that crystalline precipitate formation can be inhibited in presence of humic acid in wastewaters. Although humic acid concentration was not measured in this work, Wang and Nancollas [27] indicated that the presence of organic matter would greatly influence the crystallization of calcium phosphates.

XRD results indicated that CO_2 stripping at low pH controls calcite precipitation at the cathode, potentially increasing the recovery and purity of the fertilizer produced. Precipitates obtained using the test water which hadn't gone through Anode 1 CO_2 stripping (02/19/18 sample in Fig. 9) contained a significant amount of calcite. In contrast, the intensity of calcite peaks was reduced when the test solution underwent CO_2 stripping prior to pH shifting (02/20/18 sample in Fig. 9). The pH at which CO_2 was stripped also influenced calcite precipitation, with calcite content in the precipitates decreasing as the pH at which CO_2 was stripped was decreased. In fact, the Cathode solutions used in samples of 02/20/18 and 02/22/18 had undergone CO_2 stripping until the pH reached 4.65 and 3.93, respectively, and no calcite peaks were detected in the 02/22/18 sample. The final cathode pH of the three

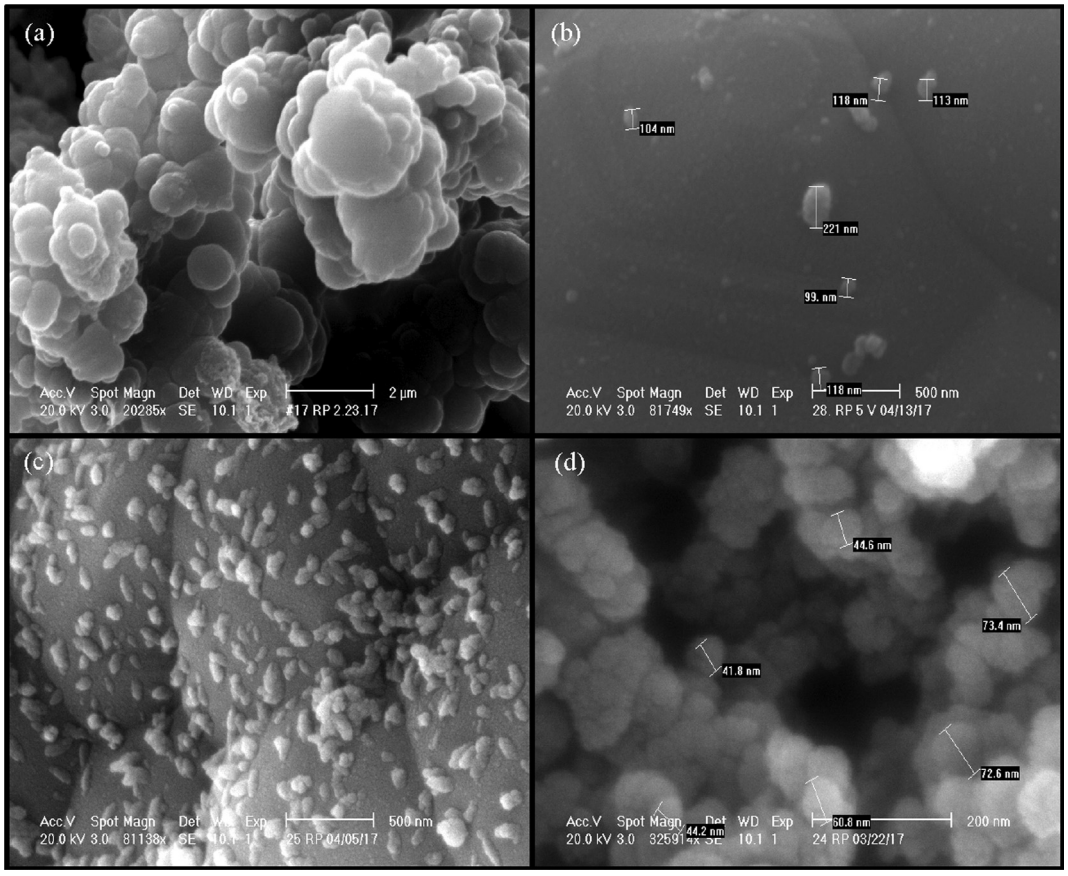

Fig. 5. Precipitates recovered from the reactor at different voltages: (a) 3.5 V, (b) 5 V (seeded), (c) 7 V (seeded), (d) 10 V [Test water: synthetic wastewater].

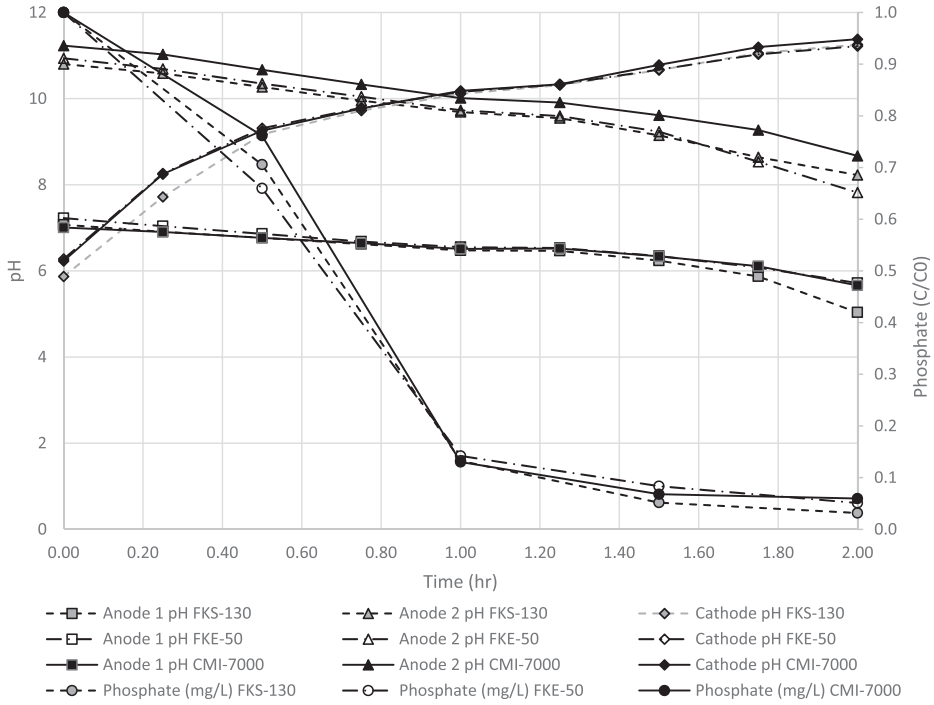

Fig. 6. Results for phosphate recovery experiments at 5 V with different multi-valent cation exchange membranes. Note: phosphate was below detection limit in the 1.5 & 2-hr samples using FKS-130, and the 2 hr sample using FKE-50. [Test water: mineral-spiked septic tank effluent; $C_{0,PO_4} = 5.64 \pm 0.22$ mg − P l^{-1}; average of triplicate results; polarity revered 5 mins every 1 hr].

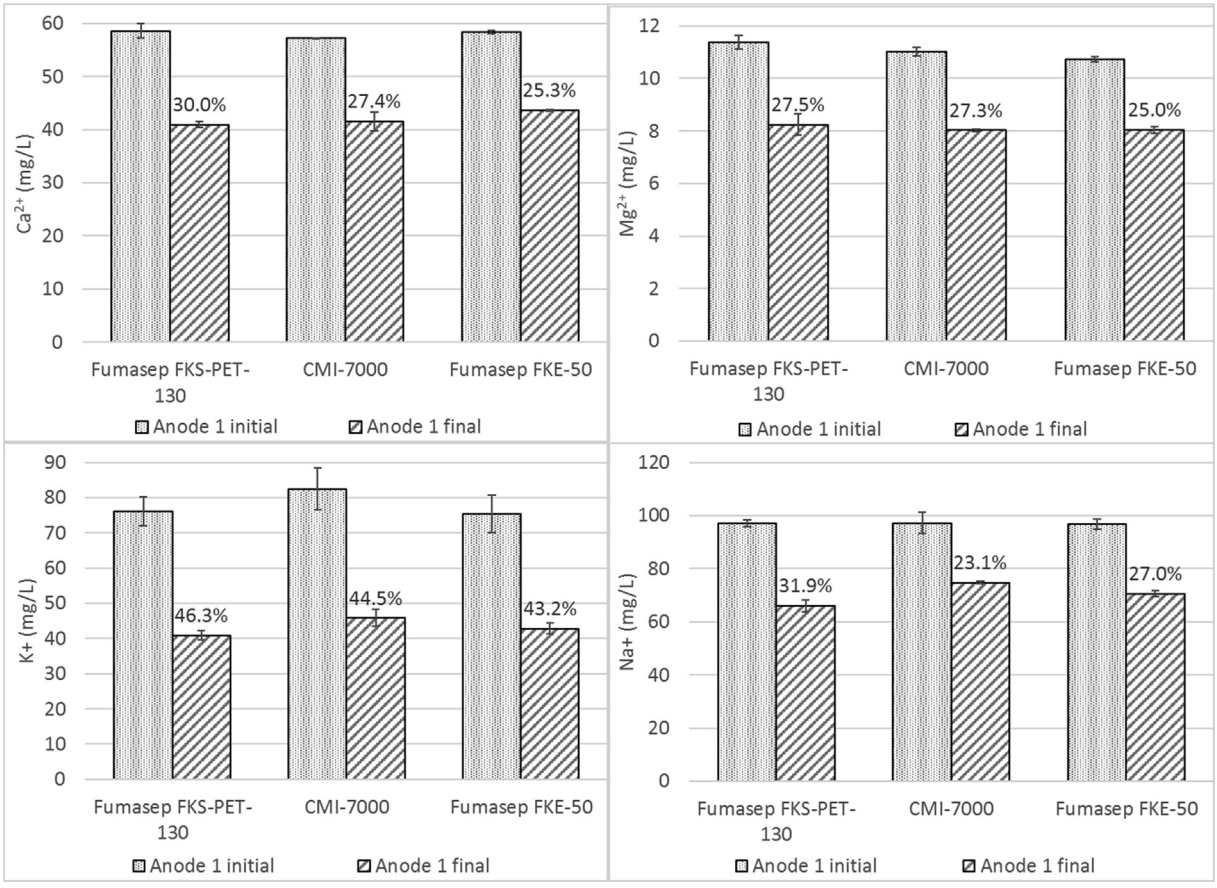

Fig. 7. Cation transportation through different MCEMs [Test water: mineral-spiked septic tank effluent].

Table 4
Phosphate Removal and Energy Consumption of Different Multi-Valent Cation Exchange Membranes Using Mineral-spiked Septic Tank Effluent.

MCEM	Average current (mA)	Current density (mA/cm^2)	Energy per 1 m^3 (kWh/m^3)	Energy per 1000 Gal (kWh/1000 Gal)	Final cathode pH	phosphate recovery %
Fumasep-FKS-130	208.9	1.3491	1.048	3.968	11.25 ± 0.15	96.8
CMI-7000	208.5	1.3467	1.046	3.960	11.38 ± 0.09	94.0
Fumasep-FKE-50	211.1	1.3634	1.060	4.012	11.22 ± 0.21	94.9

Note: Average voltage during membrane comparison experiments was 5.02 V.

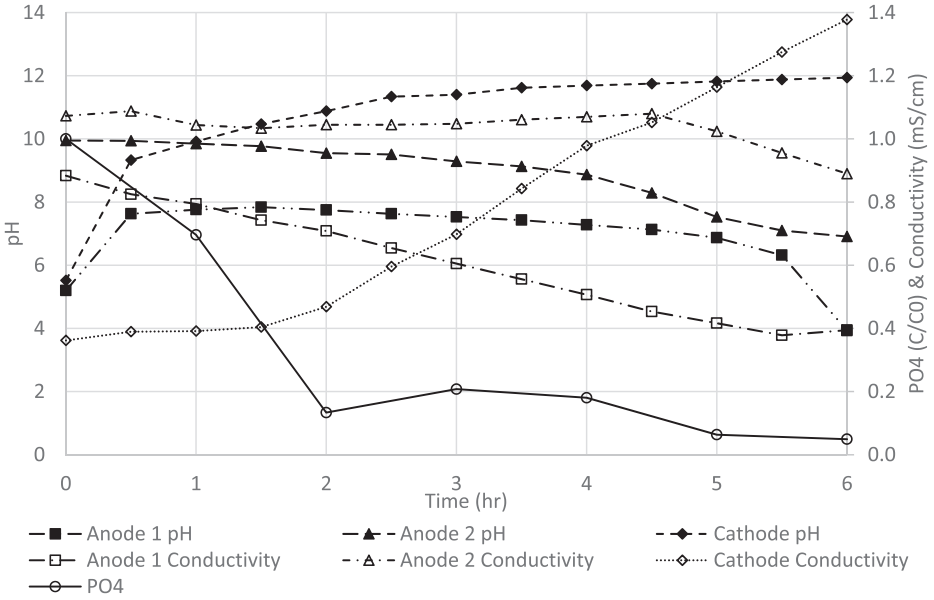

Fig. 8. Results for phosphate recovery experiments at 5 V with raw septic tank effluent [$C_{0,PO4}$ = 5.70 mg − P l^{-1}; polarity revered 5 mins after 2.5 hrs and 6 hrs].

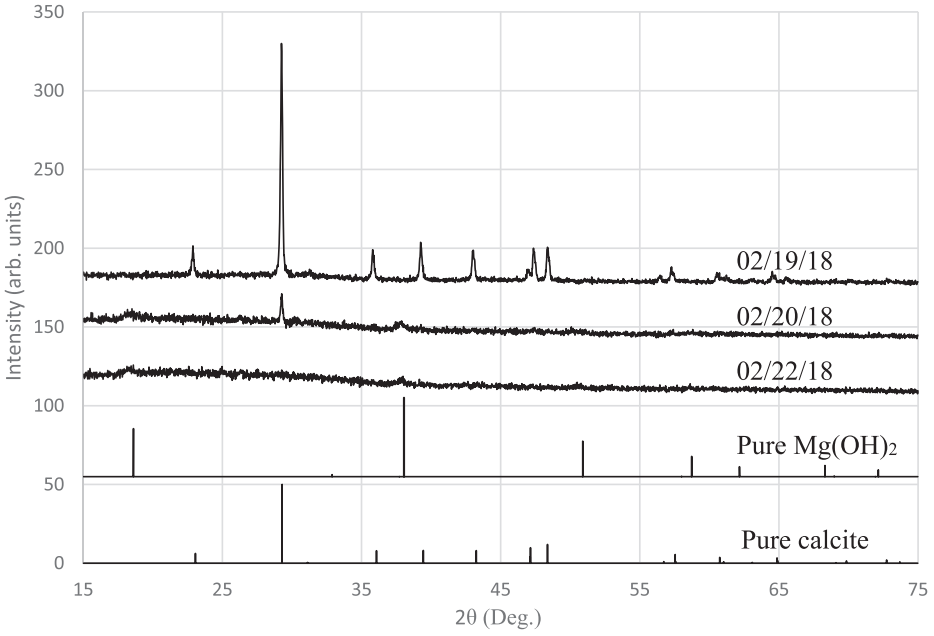

Fig. 9. X-ray powder diffraction analysis results of recovered phosphate precipitates [Test water: raw septic tank effluent, membrane: CMI-7000; voltage: 5 V).

experiments was 9.98, 11.94 and 11.87, in the samples of 02/19, 20 & 22, respectively. These results indicate that CO_2 stripping prior to pH shifting has a significant impact on the final cathode pH, with pH shifted ~ 2 pH units higher in solutions undergoing prior CO_2 stripping. Also, mild peaks of $Mg(OH)_2$ were observed in the 02/22/18 CO_2 stripped sample. In fact many authors observed $Mg(OH)_2$ precipitation at highly alkaline pH in different applications [21,28–31].

3.5. EDS analysis of precipitates

EDS analysis of the precipitates indicated that the Ca:P ratio of the recovered precipitates reached 2 as the calcite content was reduced

Table 5
Energy-dispersive X-ray Spectroscopy Analysis Results of Recovered Phosphate Precipitates [Test water: raw septic tank effluent; membrane: CMI-7000; voltage 5 V].

Element	02/19/2018	02/20/2018	02/22/2018
C	35.94	43.20	47.51
O	44.06	37.68	35.46
Na	0.12	–	–
Mg	0.44	5.53	5.40
Si	0.29	1.71	1.55
P	3.65	3.49	3.30
S	0.70	0.25	0.24
Cl	–	0.08	0.08
Ca	14.78	8.06	6.46
Sum	99.98	100.00	100.00
Ca:P ratio	4.0	2.3	2.0

through CO_2 stripping (Table 5). That is, the XRD results indicated that the calcite content of the precipitates decreased across the series of samples 02/19 > 02/20 > 02/22, and no crystalline phases of calcite were detected in the 02/22 sample. However Kappel et al. [10] indicated that the precipitates obtained in their work contained ACP and amorphous calcium carbonate (ACC), and that the Ca/P ratio increased with increasing calcium carbonate precipitation. Also, the solubility of calcium phosphates generally falls with increasing Ca/P ratio [27]; for example, brushite (Ca/P = 1) is more soluble than hydroxyapatite (Ca/P = 1.67). However, ACP, a precursor to the more stable hydroxyapatite, can have a Ca/P ratio of 1.18–2.5, and a general chemical formula of $Ca_xH_y(PO_4)_z{\cdot}nH_2O$, n = 3–4.5; 15–20% H_2O [27,32,33]. Although hydroxyapatite formation is thermodynamically favorable, it is well known that initially formed calcium phosphate does not correspond to crystalline hydroxyapatite [34]. In fact it is reported that pure hydroxyapatite is not formed even under ideal precipitation conditions [27], and reflections corresponding to hydroxyapatite were not observed in XRD analysis of the precipitates in this work (section 3.4). Considering the measured Ca/P ratio of the precipitates, the observations of Kappel et al. [10], and reported characteristics of ACP, the precipitates obtained in this work were considered to consist principally of ACP with minor amounts of calcite.

The Mg content of the precipitates in the samples of 02/20 and 02/22 increased significantly compared with that of the 02/19 sample (Table 5). This increase resulted from increased $Mg(OH)_2$ precipitation at high pH, as indicated by XRD results. At the same time, the Ca content of the samples of 02/20 and 02/22 decreased significantly compared with that of the 02/19 sample, as a result of reduced calcite precipitation. This reduced calcite precipitation was due to the fact that precipitation in the 02/20 and 02/22 experiments was carried out after anodic CO_2 stripping, which minimized alkalinity available for calcite precipitation and the associated presence of Ca in precipitates.

3.6. Solubility of the recovered P precipitate

The solubility and plant availability must be considered when assessing the agronomic value of phosphorous fertilizer. Hence, analysis of the solubility of the precipitates recovered from raw septic tank effluent was tested 3 months after precipitates were collected, resulting in a concentration of phosphate precipitates in deionized water of 13.1 mg-P l^{-1}. Because it has been reported that kinetics of transformation of ACP phases follow a “first order” rate law [27], and Christoffersen et al. [38] observed significant transformation within 4 h after ACP precipitation, it is hypothesized that phase transformation is almost completed during the 3 month period. Hence, the product appeared to stabilize with a solubility characteristic of a good slow release fertilizer (struvite solubility 21.2 mg-P l^{-1} [39]).

3.7. Voltammetry experiment results

As shown in Fig. 10, voltammetry analysis indicated that the principal reaction taking place in the test water is water electrolysis, as intended. No peaks for additional reactions were observed within the potential window of water electrolysis, 1.23 V.

3.8. Considerations for long term operation

Electrode fouling is one of the principal issues faced in electrochemical systems, and in the present process some precipitate formation was observed when the reactor was run without polarity reversal. However, no significant drop in current, or nutrient recovery efficiency, was observed. Moreover, precipitate buildup on the cathode was avoided by using the polarity reversal technique. The electrodes were used to treat raw and mineral-spiked septic tank effluent, with self-cleaning by the polarity reversal technique, and no precipitate buildup was observed over the course of 1.5 years of experimentation.

Lack of precipitate fouling during long term operation may be partially attributable to the isomolded graphite electrode material used. In particular, unlike the rare earth metal oxide coated dimensionally stable anodes (DSAs®) [10], isomolded graphite electrodes were stable under polarity reversal. Also, compared with DSAs®, isomolded graphite electrodes are inexpensive to replace. Further, the use of a non-toxic electrode material, such as isomolded graphite is important in wastewater treatment, especially in direct potable reuse applications.

4. Discussion

Regarding the value of the recovered calcium phosphate product, Bauer et al. [35] found that calcium phosphate recovered from liquid swine manure having a particle size of 0.5–1.0 mm demonstrated phosphorous plant uprate rates that was similar to commercial triple supper phosphate. Further, Van Geel et al. [36] indicated that slow release fertilizers promote the diversity of arbuscular mycorrhizal fungi, which play a key role in the functioning of agricultural ecosystems. In addition, Münch and Barr [37] indicated that slow release fertilizers have advantages including reduced nutrient loss by leaching, less frequent application requirements, and no fertilizer burn even at high application rates.

In comparison with previously reported electrochemical phosphate recovery studies, the EHM process was operated at a moderate energy demand at a low current density. Table 6 shows an energy comparison of different electrochemical phosphate recovery technologies when operated at about pH 11.

Kappel et al. [10] reported the lowest energy consumption for phosphate recovery, which is about 5 times lower than that of the EHM process (this work), though it should be noted that this reported energy demand does not include the energy demand of MBR and nanofilter operation used in that work. This low energy consumption was attributed to the platinum anode and steel cathode, which would greatly reduce the overpotential for the water electrolysis reaction but might be prohibitively expensive for municipal wastewater treatment. Further, non-mechanical electrode cleaning techniques such as polarity reversal cannot be used with steel cathodes and rare-earth metal oxide coated DSA® anodes [28]. In addition, the wastewater used in this work was highly buffered, with an average alkalinity of 183 mg l^{-1} as $CaCO_3$, whereas Kappel and coworkers used nanofiltration concentrate with an alkalinity of only 26 mg l^{-1} as $CaCO_3$.

The energy demand observed for the EHM process with the wastewater studied is significantly lower than that reported by Cid et al. [12]. This difference may be attributed to differences in the process and in wastewater composition. In the EHM process, the bulk pH is shifted, allowing phosphate precipitation in the bulk solution, whereas phosphate is precipitated on the cathode surface in Cid et al. [12]. Also, the alkalinity and chemical oxygen demand (COD) of the wastewater used

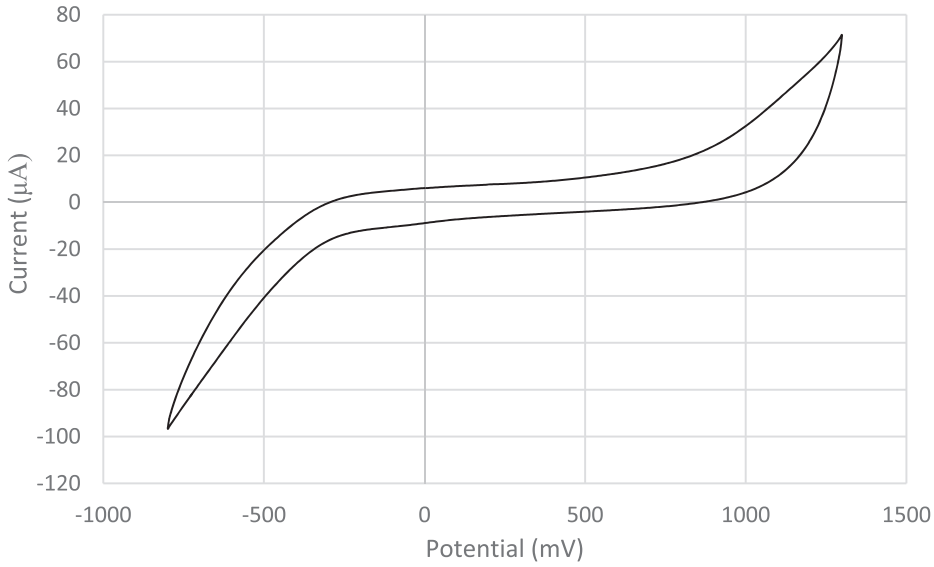

Fig. 10. Voltammetry experimental results [Synthetic wastewater; pH = 8.02; conductivity 1866 μS/cm; results plotted according to European convention].

in Cid et al. [12], 850 mg l^{-1} as $CaCO_3$ and 320–380 mg l^{-1}, respectively, were much higher than that of the septic tank effluent, 190 mg l^{-1} as $CaCO_3$ and approximately 230 mg l^{-1} COD used in EHM experiments.

Although the conductivity of the mineral-spiked septic tank effluent used in the EHM process (1414 μS/cm) was lower than that of the simulated secondary effluent Gorni-Pinkesfeld et al. [11] used in their study (1740 μS/cm), the energy used in EHM process was 177% lower than Pinkesfeld et al. [11] used in their process (2.9 kWh/m^3) to shift the pH to 11.3. Further, the EHM process was operated at a lower current density compared with the process of Pinkesfeld et al. [11], to achieve the same final cathode pH. Theoretically, the experiments of Gorni-Pinkesfeld and coworkers should have required a lower energy than the EHM process (this work), because the DSA ® anode and stainless-steel cathode used in their process would reduce the overpotential for water electrolysis reaction and higher conductivity of test water would lower the resistive losses. The low energy used in the EHM process can be attributed to reduction of buffering capability of wastewater due to prior CO_2 stripping in the Anode 1 compartment at low pH before shifting the pH in the Cathode compartment.

5. Conclusions

The electrohydromodulating phosphate recovery process designed in this work appears promising for precipitation of phosphate from mineral-spiked and raw septic tank effluent. Electrohydromodulation was carried out in a divided cell, in which the anode compartment was divided to achieve lowering of the influent pH for CO_2 stripping, subsequent raising of the pH for phosphate precipitation, and neutralization of effluent pH in a single reactor. The pH of the wastewater was shifted above 11 to remove over 90% of phosphate, and effluent pH was reduced to 8.67. The following conclusions were drawn from these results:

- Influent alkalinity played a vital role in shifting pH at the cathode, by consuming H^+ in the HCO_3^-/CO_2 equilibrium and thus buffering Anode 1 at near neutral pH, minimizing H^+ migration through the MCEM;
- Among the voltages tested in experiments with synthetic mineral-spiked septic tank effluent, 5 V and 7 V resulted in good process kinetic performance, and over 90% phosphate recovery, at energy demands of 0.934 kWh/m^3 (3.536 kWh/1000 Gal) and 1.450 kWh/m^3 (5.489 kWh/1000 Gal), respectively;
- Among the three membranes tested, the CMI-7000 CEM and Fumasep-FKS-130 were found to offer sufficient mechanical strength and high performance in terms of cation migration and pH modulation;
- 94 and 95% phosphate recovery from mineral-spiked septic tank effluent and raw septic tank effluent, respectively, were obtained using 1.046 kWh/m^3 (3.960 kWh/1000 Gal) and 1.863 kWh/m^3 (7.054 kWh/1000 Gal) of electrical energy, respectively;
- SEM, EDS and XRD analysis of the precipitates indicated that precipitates consisted primarily of ACP, with minor amounts of calcite, exhibiting an overall Ca:P ratio of 2;
- Voltammetry results indicated that water electrolysis was the only reaction taking place at the electrode solution interface, as intended;

Table 6
Energy Comparison of Electrochemical Phosphate Recovery Technologies.

Reference	Current density (mA/cm^2)	Energy per 1 m^3 (kWh/m^3)	Energy per 1000 Gal (kWh/1000 Gal)	Final cathode pH	phosphate recovery %
[10][a]	2.27	0.195[e]	1.420	11.00	96.0
[11][b]	12	2.9	10.98	11.30	96.5
[12][c]	15	~40	~151	N/A[f]	75.0
This work[d]	1.347	1.046	3.960	11.34	94.0

[a] MCEM-based electrochemical pH adjustment and precipitation from nanofiltration concentrates.
[b] MCEM-based electrochemical pH adjustment and precipitation from secondary effluent (i.e. treated wastewater).
[c] Phosphate recovery by cathodic precipitation from secondary effluent (i.e. Black water) in an undivided cell.
[d] Electrohydromodulation.
[e] Does not include the energy demand of MBR and nanofilter operation.
[f] Not applicable since bulk pH was not shifted.

and

- The inexpensive, non-toxic isomolded graphite electrodes were kinetically effective, and no fouling was observed over the course of 1.5 years of experimentation when polarity was periodically (every ~ 2 h) reversed.

CRediT authorship contribution statement

Mahamalage Kusumitha Perera: Methodology, Validation, Formal analysis, Investigation, Visualization, Writing - original draft. **James D. Englehardt:** Conceptualization, Supervision, Funding acquisition, Writing - review & editing. **Joshua L. Cohn:** . **Edward A Dauer:** . **Dharmendra Shukla:** .

Declaration of Competing Interest

The authors declare that they have no known competing financial interests or personal relationships that could have appeared to influence the work reported in this paper.

Acknowledgments

The authors would like to thank Ana Dvorak, Ebone Ross, Abigail Tinari, Kaitlyn Huaroto, and Jason Fulbright for their assistance in running the experiments and sampling, and in chemical analysis.

Funding: This work was supported by Electric Power Research Institute (EPRI Award 00-10007028), Palo Alto, California, United States.

References

[1] R.P.D. US EPA, OAR, ORIA, Radioactive Material From Fertilizer Production, (2006). https://www3.epa.gov/radtown/fertilizer-production.html (accessed February 18, 2019).
[2] M.F. Attallah, S.S. Metwally, S.I. Moussa, M.A. Soliman, Environmental impact assessment of phosphate fertilizers and phosphogypsum waste: Elemental and radiological effects, Microchem. J. 146 (2019) 789–797, https://doi.org/10.1016/j.microc.2019.02.001.
[3] P.M. Rutherford, M.J. Dudas, J.M. Arocena, Radioactivity and elemental composition of phosphogypsum produced from three phosphate rock sources, Waste Manag. Res. 13 (1995) 407–423, https://doi.org/10.1177/0734242X9501300502.
[4] J. Yang, W. Liu, L. Zhang, B. Xiao, Preparation of load-bearing building materials from autoclaved phosphogypsum, Constr. Build. Mater. 23 (2009) 687–693, https://doi.org/10.1016/j.conbuildmat.2008.02.011.
[5] A.T. Williams, D.H. Zitomer, B.K. Mayer, Ion exchange-precipitation for nutrient recovery from dilute wastewater, Environ. Sci. Water Res. Technol. 1 (2015) 832–838, https://doi.org/10.1039/C5EW00142K.
[6] M. Molinos-Senante, F. Hernández-Sancho, R. Sala-Garrido, M. Garrido-Baserba, Economic feasibility study for phosphorus recovery processes, Ambio 40 (2011) 408–416, https://doi.org/10.1007/s13280-010-0101-9.
[7] B.K. Mayer, L.A. Baker, T.H. Boyer, P. Drechsel, M. Gi, M.A. Hanjra, P. Parameswaran, J. Stoltzfus, P. Westerho, B.E. Rittmann, Total value of phosphorus recovery, Environ. Sci. Technol. 50 (2016) 6606–6620, https://doi.org/10.1021/acs.est.6b01239.
[8] M.K. Perera, J.D. Englehardt, A.C. Dvorak, Technologies for recovering nutrients from wastewater: A critical review, Environ. Eng. Sci. 36 (2019), https://doi.org/10.1089/ees.2018.0436.
[9] R. Khiewwijit, H. Temmink, H. Rijnaarts, K.J. Keesman, Energy and nutrient recovery for municipal wastewater treatment: How to design a feasible plant layout? Environ. Model. Softw. 68 (2015) 156–165, https://doi.org/10.1016/j.envsoft.2015.02.011.
[10] C. Kappel, K. Yasadi, H. Temmink, S.J. Metz, A.J.B. Kemperman, K. Nijmeijer, A. Zwijnenburg, G.J. Witkamp, H.H.M. Rijnaarts, Electrochemical phosphate recovery from nanofiltration concentrates, Sep. Purif. Technol. 120 (2013) 437–444, https://doi.org/10.1016/j.seppur.2013.10.022.
[11] O. Gorni-Pinkesfeld, H. Shemer, D. Hasson, R. Semiat, Electrochemical removal of phosphate ions from treated wastewater, Ind. Eng. Chem. Res. 52 (2013) 13795–13800, https://doi.org/10.1021/ie401930c.
[12] A. Cid, J.T. Jasper, M.R. Hoffmann, Phosphate recovery from human waste via the formation of hydroxyapatite during electrochemical wastewater treatment (2018), https://doi.org/10.1021/acssuschemeng.7b03155.
[13] T. Guo, J.D. Englehardt, Principles for scaling of distributed direct potable water reuse systems: A modeling study, Water Res. 75 (2015) 146–163, https://doi.org/10.1016/j.watres.2015.02.033.
[14] H. Huang, D. Zhang, Z. Zhao, P. Zhang, F. Gao, Comparison investigation on phosphate recovery from sludge anaerobic supernatant using the electrocoagulation process and chemical precipitation, J. Clean. Prod. 141 (2017) 429–438, https://doi.org/10.1016/j.jclepro.2016.09.127.
[15] A. Hug, K.M. Udert, Struvite precipitation from urine with electrochemical magnesium dosage, Water Res. 47 (2012) 289–299, https://doi.org/10.1016/j.watres.2012.09.036.
[16] D.J. Kruk, M. Elektorowicz, J.A. Oleszkiewicz, Struvite precipitation and phosphorus removal using magnesium sacrificial anode, Chemosphere 101 (2014) 28–33, https://doi.org/10.1016/j.chemosphere.2013.12.036.
[17] G. Chen, Electrochemical technologies in wastewater treatment, Sep. Purif. Technol. 38 (2004) 11–41, https://doi.org/10.1016/j.seppur.2003.10.006.
[18] I. Mariakakis, J. Bilbao, S. Egner, Effect of Pilot Plant Configuration on the Electrochemical Precipitation for Phosphorus recovery with the ePhos Technology, in: WEF Nutr. Symp. 2017, Fort Lauderdale, 2017: pp. 537–540.
[19] A. Adnan, M. Dastur, D.S. Mavinic, F.A. Koch, Preliminary investigation into factors affecting controlled struvite crystallization at the bench scale, J. Environ. Eng. Sci. 3 (2004) 195–202, https://doi.org/10.1139/s03-082.
[20] A. Adnan, D.S. Mavinic, F.A. Koch, Pilot-scale study of phosphorus recovery through struvite crystallization – examining the process feasibility, J. Environ. Eng. Sci. 2 (2003) 315–324, https://doi.org/10.1139/s03-040.
[21] D. Hasson, G. Sidorenko, R. Semiat, Calcium carbonate hardness removal by a novel electrochemical seeds system, Desalination 263 (2010) 285–289, https://doi.org/10.1016/j.desal.2010.06.036.
[22] Y. Jaffer, T.A. Clark, P. Pearce, S.A. Parsons, Potential phosphorus recovery by struvite formation, Water Res. 36 (2002) 1834–1842, https://doi.org/10.1016/S0043-1354(01)00391-8.
[23] Metcalf & Eddy | AECOM, G. Tchobanoglous, M. Abu-Orf, F.L. Burton, G. Bowden, H.D. Stensel, R. Tsuchihashi, W. Pfrang, Metcalf & Eddy Inc, Wastewater Engineering: Treatment and Resource Recovery, 5th ed., McGraw-Hill, New York, 2014.
[24] L.W. Gassie, J.D. Englehardt, J. Wang, N. Brinkman, J. Garland, P. Gardinali, T. Guo, Mineralizing urban net-zero water treatment: Phase II field results and design recommendations, Water Res. 105 (2016) 496–506, https://doi.org/10.1016/j.watres.2016.09.005.
[25] T. Wu, J.D. Englehardt, Mineralizing urban net-zero water treatment: Field experience for energy-positive water management, Water Res. 106 (2016) 352–363, https://doi.org/10.1016/j.watres.2016.10.015.
[26] A.E. Nielsen, Nucleation and Growth of Crystals at High Supersaturation, Krist. Und Tech. 4 (1969) 17–38, https://doi.org/10.1002/crat.19690040105.
[27] L. Wang, G.H. Nancollas, Calcium orthophosphates: Crystallization and dissolution, Chem. Rev. 108 (2008) 4628–4669, https://doi.org/10.1021/cr0782574.
[28] A. Kraft, Electrochemical water disinfection: A short review, Platin. Met. Rev. 52 (2008) 177–185, https://doi.org/10.1595/147106708X329273.
[29] H. Karoui, B. Riffault, M. Jeannin, A. Kahoul, O. Gil, M. Ben Amor, M.M. Tlili, Electrochemical scaling of stainless steel in artificial seawater: Role of experimental conditions on CaCO3 and Mg(OH)2 formation, Desalination. 311 (2013) 234–240. doi:10.1016/j.desal.2012.07.011.
[30] D. Hasson, V. Lumelsky, G. Greenberg, Y. Pinhas, R. Semiat, Development of the electrochemical scale removal technique for desalination applications, Desalination 230 (2008) 329–342, https://doi.org/10.1016/j.desal.2008.01.004.
[31] S. Zhi, S. Zhang, A novel combined electrochemical system for hardness removal, Desalination 349 (2014) 68–72, https://doi.org/10.1016/j.desal.2014.06.023.
[32] S.V. Dorozhkin, M. Epple, Biological and medical significance of calcium phosphates, Angew. Chemie Int. Ed. 41 (2002) 3130–3146, https://doi.org/10.1002/chin.200247267.
[33] R.Z. LeGeros, Formation and transformation of calcium phosphates: Relevance to vascular calcification, Z. Kardiol. 90 (2001) 116–124, https://doi.org/10.1007/s003920170032.
[34] P. Koutsoukos, Z. Amjad, B. Tomson, G.H. Nancollas, Crystallization of Calcium Phosphates: A Constant Composition Study, J. Am. Chem. Soc. 102 (1980) 1553–1557, https://doi.org/10.1021/ja00525a015.
[35] P.J. Bauer, A.A. Szogi, M.B. Vanotti, Agronomic effectiveness of calcium phosphate recovered from liquid swine manure, Agron. J. 99 (2007) 1352–1356, https://doi.org/10.2134/agronj2006.0354.
[36] M. Van Geel, M. De Beenhouwer, T. Ceulemans, K. Caes, A. Ceustermans, D. Bylemans, A. Gomand, B. Lievens, O. Honnay, Application of slow-release phosphorus fertilizers increases arbuscular mycorrhizal fungal diversity in the roots of apple trees, Plant Soil 402 (2016) 291–301, https://doi.org/10.1007/s11104-015-2777-x.
[37] E.V. Münch, K. Barr, Controlled struvite crystallisation for removing phosphorus from anaerobic digester sidestreams, Water Res. 35 (2001) 151–159, https://doi.org/10.1016/S0043-1354(00)00236-0.
[38] M.R. Christoffersen, J. Christoffersen, W. Kibalczyc, Apparent solubilities of two amorphous calcium phosphates and of octacalcium phosphate in the temperature range 30–42°C, J. Cryst. Growth 106 (1990) 349–354, https://doi.org/10.1016/0022-0248(90)90079-Z.
[39] M.I.H. Bhuiyan, D.S. Mavinic, R.D. Beckie, A solubility and thermodynamic study of struvite, Environ. Technol. 28 (2007) 1015–1026, https://doi.org/10.1080/09593332808618857.